ACS APPLIED MATERIALS & INTERFACES

Research Article

www.acsami.org

Biobutanol as Fuel for Direct Alcohol Fuel Cells—Investigation of Sn-Modified Pt Catalyst for Butanol Electro-oxidation

Vinod Kumar Puthiyapura,[†,⊥] Dan J. L. Brett,[‡] Andrea E. Russell,[§] Wen-Feng Lin,[*,†,∥] and Christopher Hardacre[*,†,⊥]

[†]Centre for the Theory and Application of Catalysis (CenTACat), School of Chemistry and Chemical Engineering, Queen's University of Belfast (QUB), Belfast, BT9 5AG, U.K.

[⊥]School of Chemical Engineering and Analytical Science, The University of Manchester, The Mill, Manchester, M13 9PL, U.K.

[∥]Department of Chemical Engineering, Loughborough University, Loughborough, Leicestershire, LE11 3TU, U.K.

[‡]Department of Chemical Engineering, University College London (UCL), London WC1E 7JE, U.K.

[§]Department of Chemistry, University of Southampton, High Field, Southampton, SO17 1BJ, U.K.

Supporting Information

ABSTRACT: Direct alcohol fuel cells (DAFCs) mostly use low molecular weight alcohols such as methanol and ethanol as fuels. However, short-chain alcohol molecules have a relative high membrane crossover rate in DAFCs and a low energy density. Long chain alcohols such as butanol have a higher energy density, as well as a lower membrane crossover rate compared to methanol and ethanol. Although a significant number of studies have been dedicated to low molecular weight alcohols in DAFCs, very few studies are available for longer chain alcohols such as butanol. A significant development in the production of biobutanol and its proposed application as an alternative fuel to gasoline in the past decade makes butanol an interesting candidate fuel for fuel cells. Different butanol isomers were compared in this study on various Pt and PtSn bimetallic catalysts for their electro-oxidation activities in acidic media. Clear distinctive behaviors were observed for each of the different butanol isomers using cyclic voltammetry (CV), indicating a difference in activity and the mechanism of oxidation. The voltammograms of both *n*-butanol and *iso*-butanol showed similar characteristic features, indicating a similar reaction mechanism, whereas 2-butanol showed completely different features; for example, it did not show any indication of poisoning. *Ter*-butanol was found to be inactive for oxidation on Pt. In situ FTIR and CV analysis showed that OH_{ads} was essential for the oxidation of primary butanol isomers which only forms at high potentials on Pt. In order to enhance the water oxidation and produce OH_{ads} at lower potentials, Pt was modified by the oxophilic metal Sn and the bimetallic PtSn was studied for the oxidation of butanol isomers. A significant enhancement in the oxidation of the 1° butanol isomers was observed on addition of Sn to the Pt, resulting in an oxidation peak at a potential ~520 mV lower than that found on pure Pt. The higher activity of PtSn was attributed to the bifunctional mechanism on PtSn catalyst. The positive influence of Sn was also confirmed in the PtSn nanoparticle catalyst prepared by the modification of commercial Pt/C nanoparticle and a higher activity was observed for PtSn (3:1) composition. The temperature-dependent data showed that the activation energy for butanol oxidation reaction over PtSn/C is lower than that over Pt/C.

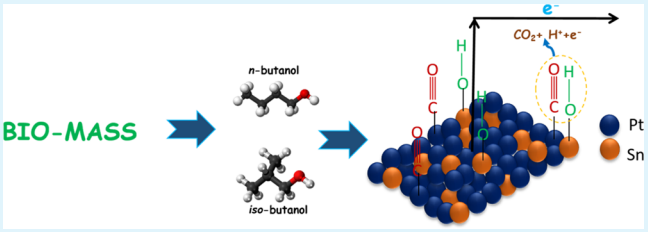

KEYWORDS: *butanol, biobutanol, direct alcohol fuel cells, electrocatalyst, PtSn, bifunctional mechanism*

1. INTRODUCTION

Direct alcohol fuel cells (DAFCs) are promising alternative power sources and have advantages over hydrogen fuel cells for portable applications. For example, DAFCs utilize liquid fuels, which increase the ease of handling and safety of the alcohol fuel.[1,2] In addition, the energy densities of low molecular weight alcohols are higher than liquid hydrogen.[1] In DAFCs, the alcohol molecule is directly oxidized on the anode, releasing protons and electrons. The electrons travel through an external circuit to the cathode side whereas the proton is transported through a proton exchange membrane (e.g., Nafion) to the cathode and reacts with the oxygen and electrons to produce water. Various alcohol molecules, such as methanol, ethanol, propanol, ethylene glycol, and glycerol, have been studied as fuels for DAFCs. However, to date, there are two major obstacles facing the development of DAFCs: (i) alcohol crossover from anode to cathode through the membrane and (ii) low activity and complex reaction mechanism of alcohol oxidation. In addition to this, the intermediates formed during the alcohol oxidation reaction, such as CO_{ads}, poison the Pt catalysts.

Received: March 7, 2016
Accepted: May 3, 2016
Published: May 3, 2016

DOI: 10.1021/acsami.6b02863
ACS Appl. Mater. Interfaces 2016, 8, 12859−12870

Methanol, being the simplest alcohol with no C−C bond, has been studied widely[2] and has been shown to be able to completely oxidize to CO_2 giving $6e^-$, but can also undergo multistep electron transfer reactions resulting in several reaction products and intermediates such as formaldehyde and formic acid. Higher alcohols which contain the C−C bonds are more difficult to oxidize as they form various adsorbed and intermediate species instead of completely oxidizing to CO_2, thus reducing the efficiency of the fuel cell.[2] For example, on a Pt electrode in acidic media, within the fuel cell operating potential range, often the number of electrons obtained for CH_3CH_2OH ($4e^-$), HCHO ($4e^-$), HCOOH ($2e^-$), *n*-PrOH ($4e^-$), i-PrOH ($2e^-$), and ethylene glycol ($4e^-$) oxidation are lower than the theoretical e^- yield for complete conversion to CO_2.[3] Ethanol has been found to oxidize predominantly by $2e^-$ and $4e^-$ pathways to give acetaldehyde (AAL) and acetic acid (AA) as the major products, respectively. The reactivity of small primary alcohols have been observed to be in the order methanol > ethanol > propanol > *n*-butanol over Pt electrode in acidic media.[4] Adsorbed CO formed as an intermediate during the alcohol oxidation, irreversibly adsorbs on Pt and acts as a catalyst poison, hindering further alcohol adsorption. Moreover, the removal of C_2, C_3, and C_4 intermediates formed during alcohol oxidation from the Pt surface is also a difficult process.[5] Therefore, the complete oxidation of alcohol fuels to CO_2 is difficult to achieve, even with state-of-the-art Pt catalysts.

A general reaction of monoalcohol oxidation in acidic media can be written as in eq 1.[2] Since an alcohol molecule contains only one oxygen atom, the complete oxidation to CO_2 requires an additional O atom, which is provided by the water or water adsorbed residue (OH_{ads})[2] formed by water oxidation on Pt. However, the oxidation of water on Pt is a difficult process and requires a high potential which increases the anodic overpotential in DAFCs.

$$C_nH_{2n+1}OH + (2n - 1)H_2O \rightarrow nCO_2 + 6nH^+ + 6ne^- \quad (1)$$

It is clear from eq 1 that as the number of carbon atoms (n) increases, the number of e^-, which can be released during oxidation also increases (e.g., 6 e^- per molecule for methanol to 24 e^- per molecule for butanol). This makes longer chain length alcohol molecules, such as butanol, interesting fuel candidates for DAFCs. In addition, the alcohol crossover rate is expected to decrease with the alcohol chain length.[6] Thus, by achieving a complete oxidation of the alcohol molecule at a lower potential, a high fuel cell efficiency could be achieved.

Various other factors such as availability, cost and sustainability also have to be considered, while selecting a suitable fuel for DAFCs. Although methanol is relatively facile to oxidation, it is toxic, flammable with low boiling point (65 °C) and is not a primary/renewable fuel and cannot be considered as an ideal fuel for practical DAFCs. In contrast, ethanol is nontoxic and can be produced by fermentation of sugars. However, the utilization of first generation biofuels produced from food-based biomass feedstock, such as bioethanol, have been the subject of significant debate over the ethics of utilizing food stock for fuel production instead of nutrition.[7] An alternate renewable source, which does not compete with the food production, is required for a sustainable energy future. Thus, second generation biofuels are proposed to be produced from nonfood based biomass feedstock such as lignocellulose biomass (LCB) (e.g., corn stover and fiber, wheat and barley straw, switchgrass, miscanthus).[7,8] The advantages of cellulose and lignin based feedstock are that they are abundant and can be considered as a waste product. In this regard, butanol is considered a second generation biofuel, with better infrastructure compatibility and higher energy density than ethanol and are superior to ethanol as a fuel itself or as a gasoline additive.[7,8] Also, biobutanol is nonpoisonous, noncorrosive, biodegradable and does not lead to soil and water pollution.[9]

Smaller chain alcohols, such as methanol and ethanol, have been widely studied as fuels for DAFCs and their electrooxidation mechanism well documented. However, butanol has been much less studied. Higher alcohols have also been studied due to the interest in the adsorption and oxidation of these molecules. The oxidation of butanol isomers on various electrodes (Pt, Au, Pd and Rh polycrystalline electrodes) in alkaline media was studied by Lamy et al.[10] They have observed that the two primary alcohols, *n*-butanol and *iso*-butanol, have a similar activity on Pt in alkaline media, whereas the secondary isomer behaves differently. The *ter*-butanol was found to be unreactive on all electrodes studied at room temperature.[10] Similar behavior was also observed by the present authors over Pt in alkaline media.[11] Since the activation of αC−H was generally identified as the initial step in the alcohol oxidation,[12] the different behaviors of the butanol isomers were assumed to be caused by the inductive effect.[13] A study on single crystal Pt electrode has shown that Pt(111) is the most active surface with lower poisoning, whereas Pt(100) and Pt(110) surfaces showed high poisoning during *n*-BtOH oxidation in alkaline media, and based on the activity the single crystal planes were classified as Pt(111) ≫ Pt(110) > Pt(100) > Pt polycrystalline.[14]

Bimetallic catalysts are generally found to be more active than the monometallic catalysts for alcohol oxidation reactions. This has been generally attributed to the bifunctional mechanism and/or ligand effect.[15] In addition, the positive effect of PtSn toward CO oxidation has been well reported in literature.[16−21] The addition of an oxophilic metal to Pt provides OH_{ads} at a lower potential than that on pristine Pt[15,22] which helps the removal of the poisoning species, CO_{ads}, by oxidizing it to CO_2. To date, PtSn was found to be the best catalyst for the ethanol oxidation reaction in acidic media.[23−29] It has been observed that nonalloyed Sn is more active in providing OH species at lower potential than the alloyed Sn[29,30] which assists in the CO_{ads} poisoning removal. PtSn was highly selective toward acetic acid formation during ethanol oxidation, whereas Pt showed selectivity toward acetaldehyde at potentials lower than that for $PtOH_x$ formation.[26,30] The CO adsorbate was found to form at lower potential on PtSn compared to that on Pt during ethanol oxidation, indicating that PtSn also activates the dissociative adsorption of ethanol.[26] DFT calculations on the PtSn system for CO oxidation showed that the CO binds only to Pt but not on Sn, whereas OH_{ads} preferentially adsorbs on the Sn sites[31] confirming the bifunctional mechanism on PtSn.

González et al.[3] reported that alcohols with H at β- carbon are readily oxidizable on PtSn electrode at lower potential than on pure Pt. They proposed that H abstraction from α and β carbon could lead to a stabilizing enol form which could then easily convert to aldehyde by the adsorbed water on Sn active sites. Zhou et al.[32] studied the single cell performance of direct ethanol fuel cell using PtSn as the anode catalysts with various Sn content. All the PtSn catalysts studied (Pt_1Sn_1/C, Pt_3Sn_2/C,

DOI: 10.1021/acsami.6b02863
ACS Appl. Mater. Interfaces 2016, 8, 12859−12870

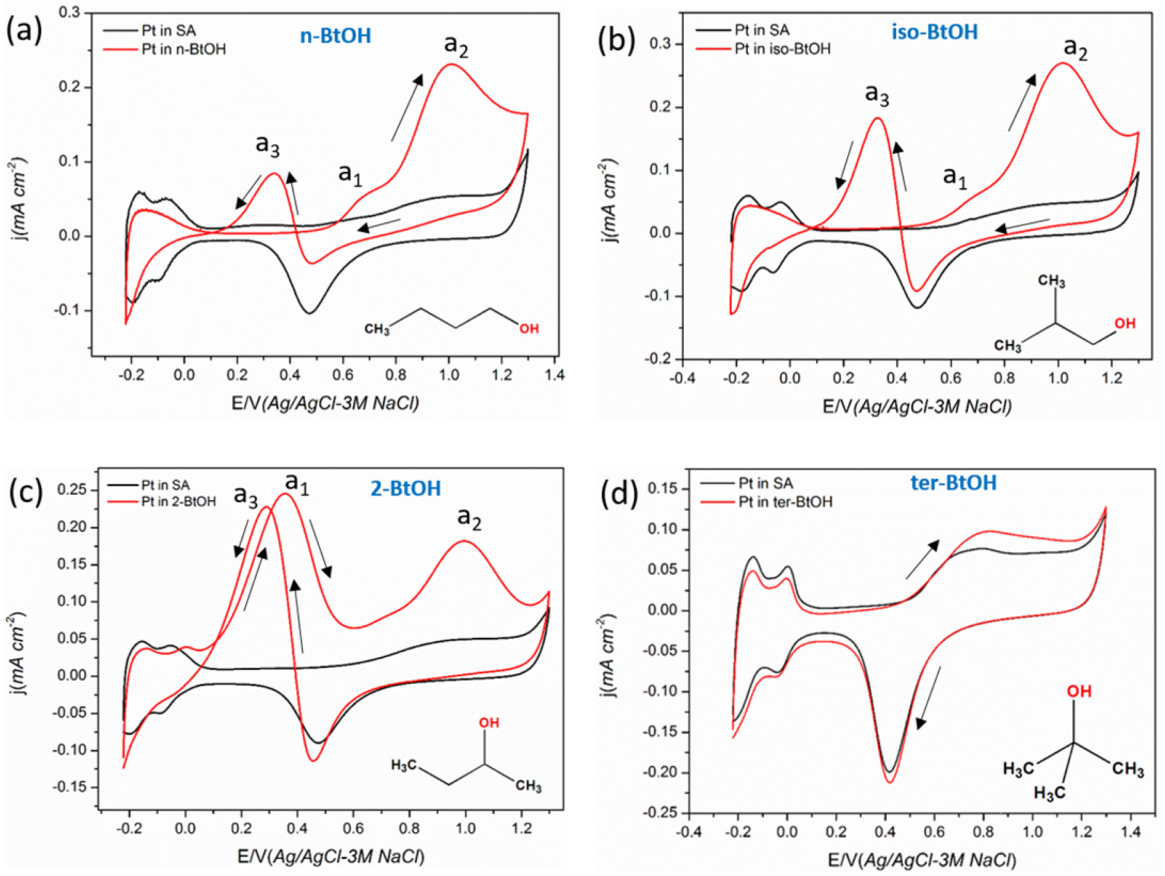

Figure 1. Cyclic voltammograms of Pt in (a) 0.1 M n-BtOH + 0.1 M H_2SO_4, (b) 0.1 M iso-BtOH + 0.1 M H_2SO_4, (c) 0.1 M 2-BtOH + 0.1 M H_2SO_4, and (d) 0.1 M ter-BtOH + 0.1 M H_2SO_4, as well as in 0.1 M H_2SO_4. Scan rate 50 mV s^{-1}, current density value was normalized by A_r of the Pt in 0.1 M H_2SO_4.

Pt_2Sn_1/C, Pt_3Sn_1/C, Pt_4Sn_1/C) showed a better performance than pure Pt, with Pt_3Sn_2 and Pt_2Sn_1 giving the maximum power density at 60 and 75 °C, respectively.

To the best of our knowledge, there are no reports on the comparison of the activity of butanol isomers on Pt in acidic media or on bimetallic catalysts. In this paper, attempt has been made to give insight into the activity of various isomers of butanol on Pt and PtSn catalysts in acidic media, building upon our previous reported data on *n*-BtOH over Pt and PtSn.[33] Both electrodeposited PtSn and Sn-modified commercial Pt/C have been studied.

2. EXPERIMENTAL SECTION

Four different isomers, *n*-butanol (Alfa Aesar, 99.4%), 2-butanol (Aldrich, ≥ 99%), *iso*-butanol (Aldrich, ≥ 99%), *ter*-butanol (Aldrich, ≥ 99%) were used as received without further purification. $H_2PtCl_6 \cdot 6H_2O$ (Alfa Aesar, ~40% Pt) and $SnCl_2 \cdot 2H_2O$ (VWR, AnalaR, NORMAPUR) were used for the catalyst preparation. All solutions were prepared using Barnstead Nanopure deionized (DI) water (resistivity 18 MΩ cm).

2.1. Synthesis of Carbon-Supported PtSn Catalysts. The carbon-supported PtSn catalysts were prepared by modifying the commercial catalyst HiSPEC-4000 Pt/C (40 wt %) catalyst with Sn using the ethylene glycol (Alfa aesar, 99%) reduction method. For this, about 300 mg of Pt/C (40 wt %) was dispersed in 30 cm^3 ethylene glycol (EG) by ultrasonication and to this, the required amount of $SnCl_2 \cdot 2H_2O$ was added to obtain the various mol % of Sn. The pH of the mixture was then adjusted to ~11−13 by using 1 M NaOH (in EG) and the mixture was refluxed at 180−190 °C for 2 h. The mixture was then cooled to room temperature slowly. The catalyst was then filtered, washed with deionized water and dried overnight in a drying oven. The catalysts prepared are denoted as PtSn (1:2), PtSn (3:1), and PtSn (2:1) based on the mole ratios of Pt and Sn. An alloy PtSn (3:1) was also prepared by the same method for comparison. In this case, H_2PtCl_6 was used as the Pt precursor and Vulcan XC-72 carbon black was used as a support. The H_2PtCl_6 and $SnCl_2$ were dissolved together and added slowly to the EG solution containing Vulcan XC-72 followed by the heat treatment and drying as explained above.

2.2. Physical Characterization. The structure of the carbon supported PtSn catalysts was investigated by powder X-ray diffraction (XRD) utilizing a Panalytical X-Pert Pro with Cu Kα radiation (λ = 1.5406 Å). The crystallite sizes of the catalyst particles were evaluated using Scherrer equation[34] from the average of the crystallite sizes of Pt(111), Pt(200), and Pt(220) planes. The surface morphology and elemental composition were studied by transmission electron microscopy (TEM) coupled with energy disperse spectroscopy (EDS) using a JEOL JEM 2100 electron microscope. The samples for TEM were prepared by adding a drop of the catalyst suspension (prepared by the ultrasonically dispersing the catalyst in ethanol) onto a Cu grid and then evaporating the ethanol. The average elemental composition was calculated from about 4−5 EDS spectra. The particle size was calculated from the TEM images (average particle size of <50−80 particles) manually using ImageJ software.

2.3. Electrochemical Analysis. The electrochemical measurements were carried out in a three electrode cell using a potentiostat (SP240, Bio-Logic). An Ag/AgCl-3 M NaCl (BaSi, USA) (0.210 V vs SHE) and a Pt mesh (Goodfellow, UK) were used as reference and counter electrodes, respectively. All potentials are referred in this article with respect to Ag/AgCl-3 M NaCl unless specified otherwise. The cyclic voltammogram (CV) analyses were carried out in 0.1 M butanol isomer +0.1 M H_2SO_4 solution. N_2 gas was passed through the electrolyte solution for 15 min before carrying out the electrochemical

DOI: 10.1021/acsami.6b02863
ACS Appl. Mater. Interfaces 2016, 8, 12859−12870

analysis. All electrodes were tested in the supporting electrolyte before testing in the butanol containing solution. The current values were normalized with the active area of Pt calculated from the hydrogen desorption area in the supporting electrolyte free from butanol.

The Pt was deposited on glassy carbon (GC) electrode (Goodfellow, UK) from 5 mM H_2PtCl_6 + 0.5 M H_2SO_4 solution at a deposition potential of −0.22 V. The electrochemical active area of Pt, A_r (in cm^2) was calculated from the CV of Pt in sulfuric acid (SA) supporting electrolyte using eq 2 where Q_H is the charge for hydrogen desorption and Q_H^o is the charge required to oxidize a monolayer of hydrogen from Pt surface (0.21 mC cm^{-2}). The current values in the CVs were normalized using A_r of Pt to give the specific current density.

$$A_r = \frac{Q_H}{Q_H^o} \tag{2}$$

The PtSn electrode was prepared by the Sn deposition onto Pt from a freshly prepared solution of 1 mM $SnCl_2$ + 0.5 M H_2SO_4 at a deposition potential of −0.21 V (the standard reduction potential of Sn(II)/Sn(0) is −0.35 V).[35,36] The Sn coverage was calculated from the CV data obtained in the supporting electrolyte, that is, the difference in the hydrogen desorption charge before and after the deposition.

For each of the carbon supported catalysts, a catalyst ink was prepared by mixing 5 mg of the catalyst with 1.5 cm^3 (ethanol + water) solvent and 20 μL Nafion solution (5 wt % solution). The latter served both as adhesive and proton conductor. The mixture was then ultrasonicated for 30 min and 10 μL ink was drop casted on to a GC electrode (7 mm diameter). The electrode was then dried at ambient temperature and electrochemical tests were carried out in the supporting electrolyte as well as in butanol containing solution.

3. RESULTS AND DISCUSSION

The CVs of Pt electrodes between the hydrogen evolution and oxygen evolution potential limits in 0.1 M H_2SO_4 showed characteristic features of Pt such as hydrogen adsorption/desorption region, double layer region, and Pt oxide formation/reduction processes (Figure 1).

3.1. Butanol Isomers in Acidic Media. In our previous study,[11] the activities of butanol isomers oxidation on Pt and Pd electrodes were studied in alkaline media and the reactivities were observed to be in the order of *n*-butanol > *iso*-butanol >2-butanol > *ter*-butanol. Herein, the activities are compared in acidic media for butanol isomer oxidation on Pt. Since the state-of-the-art fuel cells use acidic type Nafion membranes, activities in acidic media are more important from a technological perspective. The CVs of the oxidation of four butanol isomers on Pt in acidic media at room temperature are shown in Figure 1 (red in color).

Both *n*-BtOH and *iso*-BtOH (1° alcohols) showed similar oxidation profiles in the CV (Figure 1a and b), whereas 2-butanol (2° alcohol) showed significantly different oxidation features (Figure 1c). In contrast, *ter*-butanol did not show any reactivity for oxidation at all (Figure 1d). A similar trend was also observed in alkaline media on Pt and Pd previously.[11]

The *n*-BtOH and *iso*-BtOH showed two anodic peaks a_1 and a_2 (at ∼0.65 and ∼1.00 V, respectively) during the positive-going potential scan (PGPS) and one anodic peak a_3 (∼0.35 V) during the negative going potential scan (NGPS) (Figure 1a and b). These peaks are typical for the primary alcohol molecules in acidic media[1,12,37] and have been attributed to alcohol oxidation by two kinds of chemisorbed oxygen species on Pt[38] during PGPS and the reoxidation of the alcohol molecule during NGPS. It is to be noted that the characteristic CV features of Pt in acid at the hydrogen adsorption/desorption region[39] (−0.20−0.10 V) were altered in the CV of *n*-BtOH and *iso*-BtOH, indicating that some of the Pt surface active sites were covered by the adsorbates of butanol or butanol oxidation products. It is well documented that CO_{ads} is the major poisoning species formed during the oxidation of methanol and ethanol, which block the Pt active sites and prevent further adsorption of alcohol molecules onto Pt. Also, most of the primary alcohols form adsorbates that are susceptible to reduction at the potential range of the hydrogen region.[40] It was found previously that ethanol[41] and propanol[42] form ethane and propane, respectively, in addition to methane and ethane as product; this indicates that a nondissociative adsorption may also be active in the alcohol oxidation reaction.[40]

From the mechanistic studies of alcohol oxidation reactions, it is known that proton removal from the αC−H bond is the first step in the oxidation of alcohol;[13,30,38] this occurs at a low potential, leading to the dissociative adsorption of the alcohol molecule on Pt. In general, the alcohol oxidation mechanism has been described as two parallel reaction pathways (a dual-path mechanism) consisting of (i) dehydrogenation of the alcohol molecule (C−C bond cleavage) to form CO_{ads} and its further oxidation to CO_2 and (ii) the formation of an intermediate product species (without C−C bond cleavage), such as an aldehydic and carboxylic species (Scheme 1).[22,38]

Scheme 1. General Mechanism of Alcohol Oxidation on Pt Electrode[43]

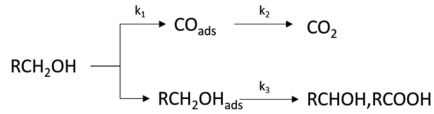

The dissociative adsorption was found to be the fastest reaction step, and generally occurs at lower potential, forming CO_{ads}. A parallel path to give intermediate species occurs with consecutive dehydrogenation steps involving C−H bonds and O−H bonds. Since the C−C bond cleavage is energetically more difficult than the C−H bond cleavage, the mechanism predominantly follows the second pathway to form partial oxidation products such as aldehyde or acid. The oxidation of these intermediate species to CO_2 is difficult and is generally considered as the rate-determining step in the overall oxidation reaction to CO_2.[5,38] In the case of butanol, C1, C2, C3, and C4 intermediate species could be formed during the oxidation.[40]

Li et al.[4,37] observed the formation of CO_{ads} at E < 0.33 V and CO_2 at E > 0.43 V during *n*-butanol oxidation on Pt in acidic media using in situ FT-IR, which indicated that the dissociative adsorption (dehydrogenation and C−C bond cleavage) of *n*-butanol occurs at the double layer region to form CO_{ads} (eq 3), which is then further oxidized at potential where Pt oxide formed (>0.43) to produce CO_2[37,44] (eq 5).

$$CH_3CH_2CH_2CH_2OH + Pt \rightarrow Pt{-}CO_{ads} + CH_3CH_2CH_3 + 2H^+ + 2e^- \tag{3}$$

The CO_{ads} formed on the Pt, blocks the active sites and inhibits further butanol adsorption.[4] This was confirmed in the present study, by varying the anodic potential limit (E_{end}) during the CV analysis of *n*-butanol oxidation (Figure 2). As the forward potential limit was increased, the reoxidation peak (peak a_3) current increases and the peak potential shifts slightly to more negative. This indicates that Pt surface was progressively

DOI: 10.1021/acsami.6b02863
ACS Appl. Mater. Interfaces 2016, 8, 12859−12870

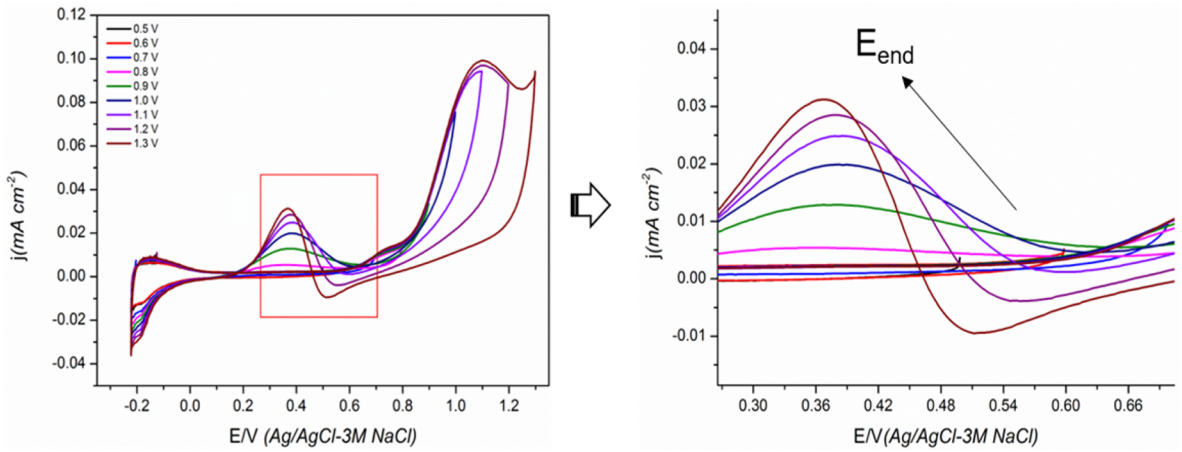

Figure 2. Effect of varying anodic potential limit on the CV of Pt/GC in 0.1 M BtOH + 0.1 M H_2SO_4 at room temperature. The anodic potential limit varied from 0.5 to 1.3 V with 100 mV increment. The cathodic potential limit was fixed at −0.22 V. Scan rate 20 mV s^{-1}.

blocked by the strongly adsorbed species and a high positive potential was required to oxidize the intermediates and clear the Pt active sites for further butanol adsorption.[13,45] At higher potentials, water is oxidized on Pt, producing OH_{ads} (eq 4) which helps in the oxidation of CO_{ads} to CO_2 (eq 5). This is clearly seen from the *n*-butanol and *iso*-butanol CV, as the oxidation of these isomers occurs only at the potential region where Pt−OH_{ads} is formed (0.50−0.75 V in Figure 1 a and b).[22]

The poisoning was also confirmed using in situ FTIR analysis (Figure S2). At $E \geq 0.50$ V, a negative feature (associated with product) appears at ∼2343 cm^{-1} in the FTIR spectra, which was attributed to the CO_2 asymmetric stretch. A further negative band at ∼3743 cm^{-1} also appears in the same potential range, which can be attributed to the OH_{ads} on Pt. It is noted that the OH_{ads} and CO_2 peaks appear at the same potential and both peaks increased with an increase in the potential, supporting the proposal that the CO_2 was produced by the CO_{ads} oxidation with the assistance of OH_{ads}. A positive peak at ∼1595 cm^{-1} also appears at potentials >0.00 V. This peak could be attributed to the consumption of water in the thin liquid layer between the CaF_2 window and the electrode.[37] The intensity of this peak increased with the increase in potential, indicating an increased consumption of water following the reaction shown in Equation 4. These results clearly validate the influence of OH_{ads} in the oxidation of alcohol molecule on Pt. Both pathways i and ii of Scheme 1 can thus occur at high potentials.[38]

$$Pt + H_2O \rightarrow Pt{-}OH_{ads} + H^+ + e^- \quad (4)$$

$$Pt{-}CO_{ads} + Pt{-}OH_{ads} \rightarrow CO_2 + Pt + H^+ + e^- \quad (5)$$

Both CO_{ads} oxidation and direct alcohol oxidation might contribute to peak a_1 for *n*-butanol and *iso*-butanol.[4] The CO_{ads} oxidation to CO_2 frees the Pt sites for further butanol adsorption which could then be oxidized to give intermediate species (peak a_2). In ethanol oxidation, the second peak is attributed to the production of acetic acid/acetaldehyde, together with some CO_2.[46,47] This incomplete oxidation was also thought to be due to C−C bond cleavage being hindered when OH_{ads} is formed on Pt.[48] Li and Sun[37] observed both CO_2 and butyric acid at potentials >0.43 V during *n*-butanol oxidation. However, the butyric acid was difficult to oxidized further to CO_2[6,37] and most of the CO_2 produced during *n*-BtOH oxidation was thus assumed to originate from the dissociative adsorption of butanol (eq 3).[37] At potentials >1.00 V, the Pt surface is covered by the oxide species (Equation 6) and leads to a decrease in the oxidation current[49,50] (Figure 1a−c).

$$2Pt{-}OH_{ads} \rightarrow Pt{-}O + H_2O + Pt \quad (6)$$

The reduction of the oxide species during the NGPS allows the reoxidation of the intermediate species formed during PGPS, as well as the oxidation of the freshly adsorbed *n*-butanol, giving rise to peak a_3. It was reported that the reoxidation peak preferentially gives the partial intermediate product rather than CO_2 for ethanol oxidation, as studied by Wang et al.[48] using differential electrochemical mass spectroscopy (DEMS). This was attributed to the poor C−C splitting rate in the potential region of peak a_3. The peak current for peak a_1 during PGPS was significantly lower than found for peak a_2, as well as a_3 indicating poor kinetics of *n*-butanol oxidation on Pt, that is, lower yield of CO_2. It has been reported elsewhere that the anodic peak current decreases with increase in the carbon chain and the activities of primary alcohols were in the order of methanol > ethanol > propanol > *n*-butanol.[1,4,51] In our previous study[11] of butanol isomers in alkaline media, the primary isomers showed an increase in oxidation current just after the hydrogen desorption region, indicating the effect of OH_{ads} on the alcohol oxidation as the Pt surface was already covered by OH_{ads} in the hydrogen region in alkaline media. Also here, the ratio of the peak a_2 to peak a_1 is higher for *n*-butanol and *iso*-butanol compared to that for 2° alcohol, which could indicate that for 1° butanol isomers, the direct oxidation pathway of alcohol could be more prominent relative to the CO pathway.[46] In alkaline media, the peak a_2 to peak a_1 ratio was significantly lower[11] indicating direct alcohol oxidation pathway is less prominent. In alkaline media, kinetic factors may improve the efficiency of the CO route due to easy OH adsorption. This could decrease the direct oxidation of alcohol molecules, whereas the CO route will be unaffected.[46] In order to make use of the fuel in a fuel cell, a complete conversion to CO_2 has to be achieved by making the reaction mechanism preferentially follow the CO pathway at a lower potential. From the above results, it is clear that for primary alcohols, the CO pathway is less prominent but occurs at lower potential, whereas the partial oxidation pathway is dominant and occurs at higher anodic potential.

DOI: 10.1021/acsami.6b02863
ACS Appl. Mater. Interfaces 2016, 8, 12859−12870

In contrast to the 1° butanol isomers, the 2° alcohol, 2-butanol, showed quite a different CV feature (Figure 1 c). Two oxidation peaks were observed during PGPS and one oxidation peak during NGPS. The oxidation current increased just after the hydrogen desorption region during the PGPS, giving rise to a peak at ~0.35 V (peak a_1) and another peak at ~1.00 V (peak a_2). During NGPS, an oxidation peak was observed at ~0.30 V (peak a_3). The peak a_1 could be attributed to the dehydrogenation of 2-butanol, whereas peak a_2 could be due to the direct oxidation of 2-butanol.[52] The hydrogen desorption region was not suppressed as much as *n*-butanol and *iso*-butanol, which indicates that the dissociative adsorption (C−C bond breaking) did not occur for 2-butanol to form strongly adsorbed intermediates such as CO_{ads}.[13,49,53] Thus, oxidation of 2-butanol occurs once the hydrogen is desorbed from the Pt surface. It is clear that the 2° alcohols have a different oxidation mechanism compared to the 1° alcohols. This might indicate a relatively high activation energy requirement for the C−C bond cleavage in 2° alcohols compared to the 1° alcohols.[50] An absence of CO_{ads} during 2° alcohol oxidation has been reported for 2-propanol oxidation based on FT-IR analysis[44,54−56] whereby acetone and CO_2 were the major products,[54,57] albeit with CO_2 only formed in negligible amounts.[57] The FTIR analysis of 2-butanol on Pt showed similar features, as found during n-BtOH oxidation with the CO_2 peak appearing in potential region where Pt−OH/O_x was formed (Figure S4), indicating that peak $\mathbf{a_1}$ is not associated with CO_2 formation and could be a direct oxidation of 2-butanol, as mentioned above. It is worth pointing out that the formation of ketone species from 2° alcohol does not require water and thus direct oxidation can occur before the water oxidation occurs on Pt.[57] Oxidation of 2-butanol to 2-butanone can occur as given in eq 7.

$$CH_3CH_2CH(OH)CH_3 \rightarrow CH_3CH_2(CO)CH_3 + 2H^+ + 2e^- \quad (7)$$

During the NGPS, a reoxidation peak was observed, as in the case of *n*-BtOH and *iso*-BtOH, in a similar potential region and can be attributed to the reoxidation of the butanol molecule.[38] On increasing the anodic potential limit, oxidation current peaks a_1, a_2, and a_3 all increased for 2-butanol (Figure S3). A negative potential shift of the peak a_3 was also observed, indicating the formation of PtO_x and blocking of alcohol adsorption at the higher potentials. A more negative potential was required to reduce the PtO_x formed at higher potentials and then the surface could be freed up for further fuel adsorption and oxidation. When the potential limit was lower than the PtO_x formation region (<~0.70 V), both peak a_1 and a_3 superimpose, indicating a reversible reaction, confirming the lack of poisoning of Pt electrode during 2-BtOH oxidation.[49] As the potential was increased beyond the PtO_x region, the intermediates were oxidized and the reduction of Pt oxide during NGPS, which released the Pt sites free for further 2-butanol adsorption and oxidation. This resulted in the increased NGPS oxidation peak current density and also explained its peak potential shift. On Pt and Pd in alkaline media, 2-butanol showed a lower onset potential as well as multiple oxidation peaks during PGPS.[11] But in contrast to acidic media, the oxidation current was significantly lower for 2-butanol in alkaline media in comparison to the 1° alcohols showing the influence of the electrolyte media on the oxidation mechanism for 2-butanol.

Ter-butanol did not show any reactivity toward oxidation and the CVs were similar to that of Pt in the acidic supporting electrolyte at room temperature (Figure 1 d). However, a small improvement in the *ter*-butanol oxidation activity on Pt at high temperature in acidic media has been reported elsewhere.[12] The inactivity of *ter*-butanol is anticipated, as no αC−H bond is present in *ter*-butanol which is the first step in the oxidation of alcohol molecules. A similar inactivity of *ter*-butanol was also observed in alkaline media on Pt and Pd.[11] A lower activation energy of 2.1 kJ mol^{-1} for 2-butanol oxidation on Pt/C microporous electrode in acidic media (at the first anodic peak of ~0.35 V) compared to the first anodic peaks for ethanol (22.1 kJ mol^{-1}) and 2-propanol (10.4 kJ mol^{-1})[49] has been reported, indicating facile reaction kinetics for 2-butanol oxidation. This indicates that the long chain 2° alcohols can give better performance, even without C−C bond cleavage, but the complete oxidation to CO_2 does not occur at lower potential as they follow the nondissociative pathway. On the other hand, for 1° alcohol, the partial oxidation occurs at high potential only as the CO formed by dissociative adsorption blocks the Pt sites at a lower potential.

The peak current of a_1 can generally be correlated with the oxidation activity of the alcohol molecule. On the basis of this, it is clear that both 1° and 2° isomers on Pt in acidic media have a similar activity. 2-Butanol, on the other hand, showed a higher current for peak a_1 than the 1° alcohol. However, the peak a_1 for 2-butanol oxidation is associated with a partial oxidation reaction without involving C−C bond cleavage, which thus reduces the conversion efficiency of 2-butanol when used as fuel. *Ter*-butanol, show no activity for oxidation on Pt. The activity of the butanol isomers for oxidation on Pt in acidic media can thus be given in the order 2-BtOH > *n*-BtOH> *iso*-BtOH ≫ *ter*-BtOH.

Thus, it is clear that 1° isomers are potentially more active for oxidation to give completely oxidized product CO_2 at a lower potential, but the CO_2 production is inhibited by the poisoning species CO. The FTIR and CV analysis indicate that OH_{ads} is essential for the CO oxidation and to release Pt sites. Modification of the Pt-based catalyst to provide OH_{ads} at lower potentials has the potential to effectively oxidize the 1° alcohols to give CO_2. This strategy, however, may not be relevant to 2-butanol, where the mechanism follows a different pathway at lower potentials without CO_{ads} formation. The addition of oxophilic metals to Pt were reported to enhance the alcohol oxidation reaction.[15,22] This was explained by the ability of the oxophilic metal to oxidize water at lower potential, providing OH_{ads} species in comparison to bare Pt, where a high overpotential is required for H_2O oxidation (bifunctional mechanism). The activity for chemisorption of water for various metals are in the order Cu < Pd < Rh < Pt < Ru < Sn.[58] As Sn is the most active metal for water decomposition, a PtSn bimetallic system was studied for butanol oxidation, herein.

3.2. PtSn Bimetallic Catalyst for Butanol Isomer Oxidation in Acidic Media. In our previous study,[33] a higher activity of PtSn than Pt for *n*-butanol oxidation in acidic media was reported. Here, the reactivity of PtSn for the electrooxidation of all four butanol isomers was compared to Pt in acidic media. Sn was electrodeposited on Pt as described in the Experimental Section. The Sn, especially on the surface, is likely to be mostly present as oxide[3,59] because of the exposure to atmosphere, as well as the charge transfer from Sn to Pt caused by the electronegativity difference between the two metal atoms.[5,21,30,60]

DOI: 10.1021/acsami.6b02863
ACS Appl. Mater. Interfaces 2016, 8, 12859−12870

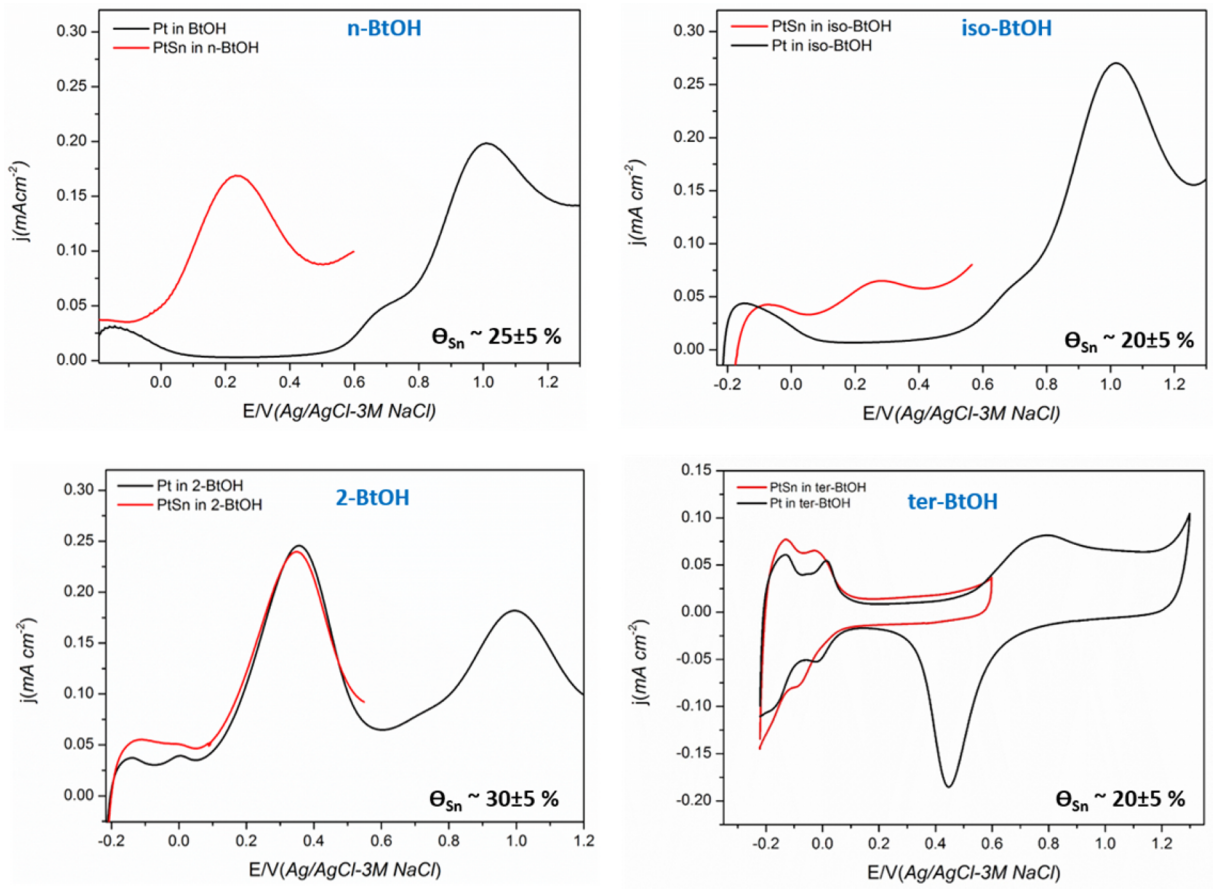

Figure 3. CVs of Pt and PtSn in solutions of 0.1 M butanol isomer +0.1 M H_2SO_4: (a) *n*-butanol, (b) *iso*-butanol, (c) 2-butanol, and (d) *ter*-butanol. The current values were normalized by A_r of Pt for both Pt and PtSn electrodes. The Sn coverage (θ_{Sn}) is also given in the respective figure.

The morphology of the Pt was not modified significantly by the Sn addition and a spherical cauliflower type of morphology of Pt was preserved for PtSn, as reported in our previous study.[33] The current density value for PtSn electrodes was normalized by the A_r calculated from the CV of PtSn in 0.1 M H_2SO_4. The composition of PtSn was difficult to determine from EDX and XRD analysis due to the low Sn coverages, and also, it is likely that not all the Sn is being present in crystalline form.[21] Thus, the Sn coverage (θ_{Sn}) was calculated using the electrochemical method from the difference in the hydrogen desorption charge before (Q_H) and after the Sn deposition (Q_H^{Sn}), as given in eq 8.[21] This method also allows the determination of the active area without modifying the Pt−Sn surface before testing it in butanol solution. Suppression of the hydrogen desorption region, as well as an increased double-layer current for the PtSn (because of the oxide formation) electrode, is consistent with the presence of Sn on Pt (Figure S5). This method has been reported in literature to estimate the Sn coverage on Pt.[21,33,35,59]

$$\theta_{Sn} = \frac{Q_H - Q_H^{Sn}}{Q_H} \quad (8)$$

During the PGPS in H_2SO_4 (Figure S5), an oxidation peak appears with an onset potential of ∼0.15 V and the peak potential at ∼0.50 V for PtSn, indicating the oxidation of adsorbed Sn species by the dissociation of water on Sn.[21,39,59] A small reduction peak at ∼0.35 V could be attributed to the reduction of oxidized Sn, as at the upper potential in the CV, Pt surface is not oxidized.[59] The upper potential in CV analysis was limited to a maximum of 0.60 V for PtSn to avoid dissolution of Sn into solution at higher potentials.[61] The lower onset potential of tin oxidation (∼0.15 V) than the Pt oxidation potential (∼0.55 V) also confirms the oxophilic nature of Sn.

Figure 3a shows the PGPS of the Pt and PtSn electrode in 0.1 M *n*-BtOH + 0.1 M H_2SO_4 solution. The Pt shows characteristic features of butanol oxidation with an onset potential of ∼0.55 V.[33] However, for the PtSn electrode, a peak at lower potential of ∼0.27 V was observed which is at significantly lower potential than the peak a_1 for Pt (∼0.65 V). Similar behavior was also observed for *iso*-butanol (Figure 3 b). This lower potential peak was not observed in the supporting electrolyte (0.1 M H_2SO_4), but only in *n*-butanol and *iso*-butanol containing solutions, indicating that the peak originated from the butanol oxidation. This was also further confirmed by gradually adding *n*-butanol to 0.1 M H_2SO_4 supporting electrolyte while running the CV, the lower potential peak appears only when butanol was added to the solution (not shown). Since this peak appears at a potential region far below $PtOH/PtO_x$ formation, the active oxygen species for the *n*-BtOH and *iso*-BtOH must originate from the Sn. The oxygenate species formed on Sn could be either an OH_{ad} species or the SnO_2 itself.[25] This may be attributed to the low onset potential for OH_{ads} formation on Sn as observed previously.[25,62] A similarity between the primary butanol on PtSn and 2-butanol on Pt is notable. Both show an increase in oxidation current after the hydrogen desorption region, indicating that poisoning is not dominant and the oxidation

DOI: 10.1021/acsami.6b02863
ACS Appl. Mater. Interfaces 2016, 8, 12859−12870

of the alcohol occurs in this potential region. A similar lower potential peak at ~0.23−0.29 V was also observed for ethanol oxidation on PtSn[25,30,33,62] and methanol oxidation on PtRu.[15] In addition to the lower onset potential, a higher current efficiency of CO_2 production was also observed on PtRu and PtSn for the methanol oxidation reaction and was attributed to electronic modification of Pt by Ru in addition to the bifunctional mechanism.[15] It is noted that the onset for *n*-butanol and *iso*-butanol oxidation on PtSn was at significantly lower potential (~0.0−0.05 V) compared to that on Pt (~0.55 V). A lower onset of 150−300 mV for CO oxidation on PtSn compared to Pt was observed in CO stripping experiments,[21,26] confirming the positive effect of Sn on the CO oxidation reaction on Pt. Also, a lower onset potential of about 100−200 and 200−300 mV, respectively, for methanol[39] and ethanol[25,26,33] oxidation on PtSn compared to Pt has been reported and explained by the bifunctional mechanism. The Sn adsorbs oxygenated species at lower potentials leading to the easy removal of strongly adsorbed CO_{ads} as given in eq 9−12,[25,26] which helps in the further adsorption of butanol. This is a significant observation as it indicates that even long chain alcohol, such as butanol, could be effectively oxidized on bimetallic PtSn catalyst, at even lower potential than ethanol on Pt electrode.

$$SnO_2 + H_2O \rightarrow SnO_2{-}OH_{ads} + H^+ + e^- \quad (9)$$

$$Sn + H_2O \rightarrow Sn{-}OH_{ads} + H^+ + e^- \quad (10)$$

$$Pt{-}CO_{ads} + SnO_2{-}OH_{ads} \rightarrow CO_2 + H^+ + e^- \quad (11)$$

$$Pt{-}CO_{ads} + Sn{-}OH_{ads} \rightarrow CO_2 + H^+ + e^- \quad (12)$$

The effect of temperature on *n*-butanol oxidation on electrodeposited Pt and PtSn electrodes was reported in our previous work[33] and a lower activation energy on PtSn compared to Pt was observed at the oxidation peak region. González[3] observed that alcohols with H atoms on the β carbon can be oxidized on PtSn at lower potential than on Pt. They proposed that H abstraction from α and β carbons could lead to the formation of a stabilizing enol structure which could then convert to an aldehyde. This conversion would be facilitated by the O-rich surface of the Pt−Sn, as the attack on enol by adsorbed H_2O could easily form a hydrated aldehyde.[3]

It was observed in our previous experiments on *n*-butanol oxidation that, at high Sn coverage (>40%), the anodic peak current at ~0.60 V was suppressed significantly[33] and was assumed to be the blocking of Pt active sites by the Sn adatoms.[15] However, with an increase in number of cycles between the potential ranges −0.22 to 0.75 V, the peak at ~0.60 V starts to appear, indicating that dissolution of Sn may be occurring at higher potentials, freeing up the Pt active sites for butanol adsorption. It is obvious that the Pt active sites are required for the butanol adsorption as Sn does not adsorb CO[31] but only helps in the water adsorption at low overpotentials.[21]

The PtSn electrode for the oxidation reaction of *iso*-butanol also showed a similar feature to that of *n*-butanol (Figure 3b), whereas 2-butanol and *ter*-butanol did not show any significant activity on the PtSn electrode. As discussed previously for the Pt electrode, CO_{ads} was not formed from 2-butanol and thus no significant improvement was observed on PtSn compared to Pt. Similar behavior was also observed for 2-propanol oxidation on PtRu with no difference in the activity compared to pure Pt.[52] The inactivity of *ter*-butanol on PtSn has also been reported.[3] As discussed in the previous section, the primary isomers of butanol are more active for the oxidation reaction, but the CO poisoning increases the overpotential. It was clear from this study that using bimetallic catalyst such as PtSn, the poisoning species can be removed at lower potential and thus can facilitate the oxidation of butanol at a lower potential.

3.3. Carbon-Supported PtSn Catalyst for *n*-Butanol Oxidation. To further confirm the Sn effect on Pt for butanol oxidation, and also to control the Sn composition more accurately, commercial Pt/C (40%) was modified by Sn using a chemical reduction method described in the Experimental Section. The XRD spectra of the PtSn/C catalysts are given in Figure 4. The XRD shows typical peaks for the face centered cubic (fcc) structure of crystalline Pt.[63] The particle size of Pt was in the range of ~4.1−4.4 nm for all the samples and was calculated using the Scherrer equation.[34] Only PtSn with high Sn content showed Sn related peaks in the XRD which were not observed at low Sn contents.[32] For the higher Sn loaded materials, two peaks with the 2θ at ~34° and ~53° were observed which may be associated with the SnO_2 phase.[63−65] However, these peaks were relatively broad, which could indicate the amorphous nature of Sn as the catalysts were used as prepared and not subjected to further heat treatment.

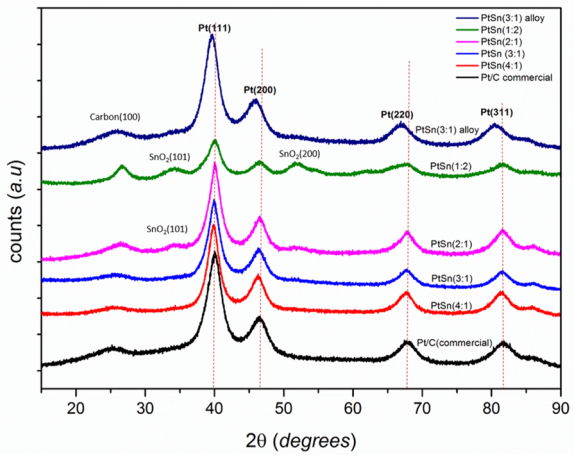

Figure 4. XRD spectra of the PtSn/C nanoparticles. Of which PtSn(1:2) and PtSn(2:1) showed peaks for SnO_2 as well.

For the PtSn (3:1)-alloy catalyst, all the diffraction peaks were slightly shifted to lower 2θ values compared to the Pt/C (40%), which confirm alloy formation;[5,25] whereas for all other Sn-modified Pt/C catalysts, no such peak shifts were observed, confirming the nonalloy nature of the PtSn particle, as expected. Also the particle size for the alloy was lower than that of the Sn modified Pt/C catalysts, which is typical for alloy catalysts.[25] The BET surface areas of these catalysts were not significantly different after Sn addition, although a slight increase in the surface area was observed with increase in Sn content for the PtSn/C catalysts (Table 1). The alloy catalyst, on the other hand, showed a higher surface area than all other catalysts, which may explain the slightly greater current density associated with the PtSn(3:1) alloy catalyst (Figure S6) compared to the Sn modified PtSn(3:1) catalyst.

The TEM images of the PtSn(3:1) and PtSn(2:1) are given in Figure 5. A uniform distribution of the spherical particles on the carbon support is evident from the TEM. The average

DOI: 10.1021/acsami.6b02863
ACS Appl. Mater. Interfaces 2016, 8, 12859−12870

Table 1. Physical Properties of the PtSn Nanoparticle Catalysts Studied[a]

catalyst	Sn (mol %) theoretical	average Sn (mol %) from EDX	crystallite size of Pt from XRD (nm)	BET surface area (m^2 g^{-1})	average particle size from TEM (nm)
Pt/C (40%) commercial	0		3.7	140	
PtSn (1:2)	66.6	68.5	4.1	143	3.0
PtSn (2:1)	33.3	36.5	4.4	143	4.2
PtSn (3:1)	25	24.5	4.4	134	3.2
PtSn (4:1)	20	23	4.4	133	3.5
PtSn (3:1) alloy	25	25.4	3.6	159	3.9

[a]Crystallite size was calculated from the average of the crystallite size of Pt(111), Pt(200) and Pt(220) planes. Sn mol % calculated from the average of 4−5 EDS spectra.

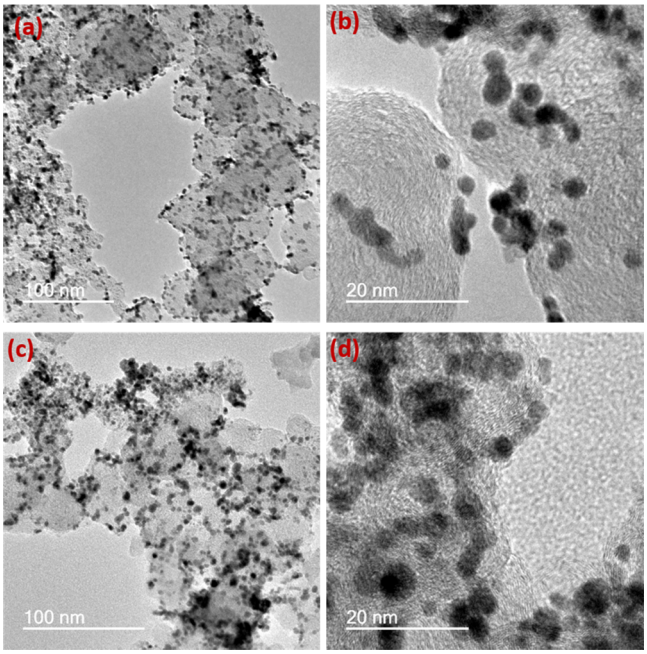

Figure 5. TEM images of (a, b) PtSn(3:1)/C and (c, d) PtSn (2:1)/C nanoparticles.

particle size from TEM and XRD was similar, with a slightly higher value obtained from XRD. This could be due to the fact that the TEM particle size was calculated from the average 50−80 clearly distinguishable particles, whereas XRD represents the bulk sample and the response is dominated by the large crystallites present. An EDS analysis was also carried out for the TEM samples and the compositions obtained for the various samples are given in Table 1. The composition obtained was more or less similar to that expected. However, the possibility of some Sn being deposited on carbon cannot be discarded.

The PGPS voltammogram of PtSn/C nanoparticles in *n*-butanol-containing solution is compared in Figure 6. For all PtSn catalysts, an oxidation peak between 0.1−0.3 V was observed as found for the electrodeposited PtSn catalyst in Figure 3. However, the current density was found to vary with the composition of the catalysts. The maximum current density for the lower potential peak was found for PtSn(3:1). This could be the result of the Pt active sites being blocked by excess Sn for butanol adsorption at higher Sn contents;[32] whereas, at lower Sn content, there was not sufficient OH_{ads} species on Sn sites for CO_{ads} oxidation. Thus, it may be assumed that there is an optimum Sn coverage required for an effective butanol oxidation. The PtSn electrodeposited catalyst also showed a higher current for ∼25% coverage and thus about 20−30% Sn could be considered as an optimum Sn content for the PtSn catalyst. The PtSn(3:1)-alloy catalyst also showed a clear lower potential peak (Figure S6), confirming this assumption. A slightly higher peak current was observed for PtSn(3:1)-alloy catalyst (Figure S6) compared to the nonalloyed catalyst (Figure 6b), which is in contrast with some of the previous reports, where poor activity has been observed for alloy PtSn catalysts, and had been attributed to the electronic interaction between Pt and Sn in the alloy phase.[25,66] On the contrary, the electronic effect can also be advantageous, as the charge transfer to Pt by Sn can weaken the Pt-CO bond, which helps in the removal of CO as to be oxidized to CO_2.[67,68] Silva et al.[69] observed a higher current density during ethanol oxidation for PtSn/C alloy catalyst compared to the nonalloyed one which was attributed to the CO_2 formation with slow kinetics on nonalloyed catalyst vs acetic acid formation with faster kinetics for alloyed catalyst. However, as mentioned before the higher surface area could also be the reason for the higher current in the case of alloy catalyst. Further studies are required to clearly distinguish the difference in activity/mechanism in alloy and nonalloyed catalyst.

The Arrhenius plots of the butanol oxidation on Pt/C (40%) commercial catalyst and PtSn(3:1) are given in Figures S7 and S8. The activation energy for *n*-butanol oxidation on PtSn(3:1) at 0.20 and 0.30 V was significantly lower (15 kJ mol^{-1}) than found for Pt/C (40%) at 0.62 V (37 kJ mol^{-1}). Similar results were also observed for electrodeposited PtSn in our previous study.[33] Since the first peak on Pt is attributed to the butanol oxidation after the removal of CO_{ads} species, the lower activation energy on PtSn can be attributed to the effectiveness of the catalyst in CO_{ads} removal by the bifunctional mechanism which helps in the adsorption of butanol molecules on Pt. An increase in the lower potential oxidation peak current with increase in *n*-butanol concentration was observed for PtSn(3:1)/C (Figure S9). Also, with increase in the BtOH concentration, the peak becomes more distinguishable at higher BtOH concentration. A similar behavior was also reported for ethanol oxidation reaction on PtSn.[70] All of these confirm the fact that the lower potential peak originates from the butanol oxidation reaction.

4. CONCLUSIONS

A series of long chain C4 alcohols have been studied for electrochemical oxidation in acidic media on a Pt electrode. It was demonstrated that the different butanol isomers behave differently in their electrochemical oxidation. Both 1° alcohols, *n*-butanol and *iso*-butanol, have a similar reactivity for oxidation, whereas 2-butanol, a 2° alcohol, is quite different in its electrochemical oxidation behavior. This indicates a difference in the mechanism of the 1° and 2° isomers. From the CV and FTIR results, it was proposed that 2-butanol does not undergo C−C bond cleavage and thus not produce poisoning species such as CO_{ads}. The oxidation current was also higher for 2-butanol compared to that of 1° alcohols, indicating its effectiveness in oxidation without C−C cleavage to give partial oxidation products, though the partial oxidation will reduce the conversion efficiency of the fuel. The *ter*-butanol, on the other hand, is not reactive for oxidation at all. The 1° and 2° isomers

DOI: 10.1021/acsami.6b02863
ACS Appl. Mater. Interfaces 2016, 8, 12859−12870

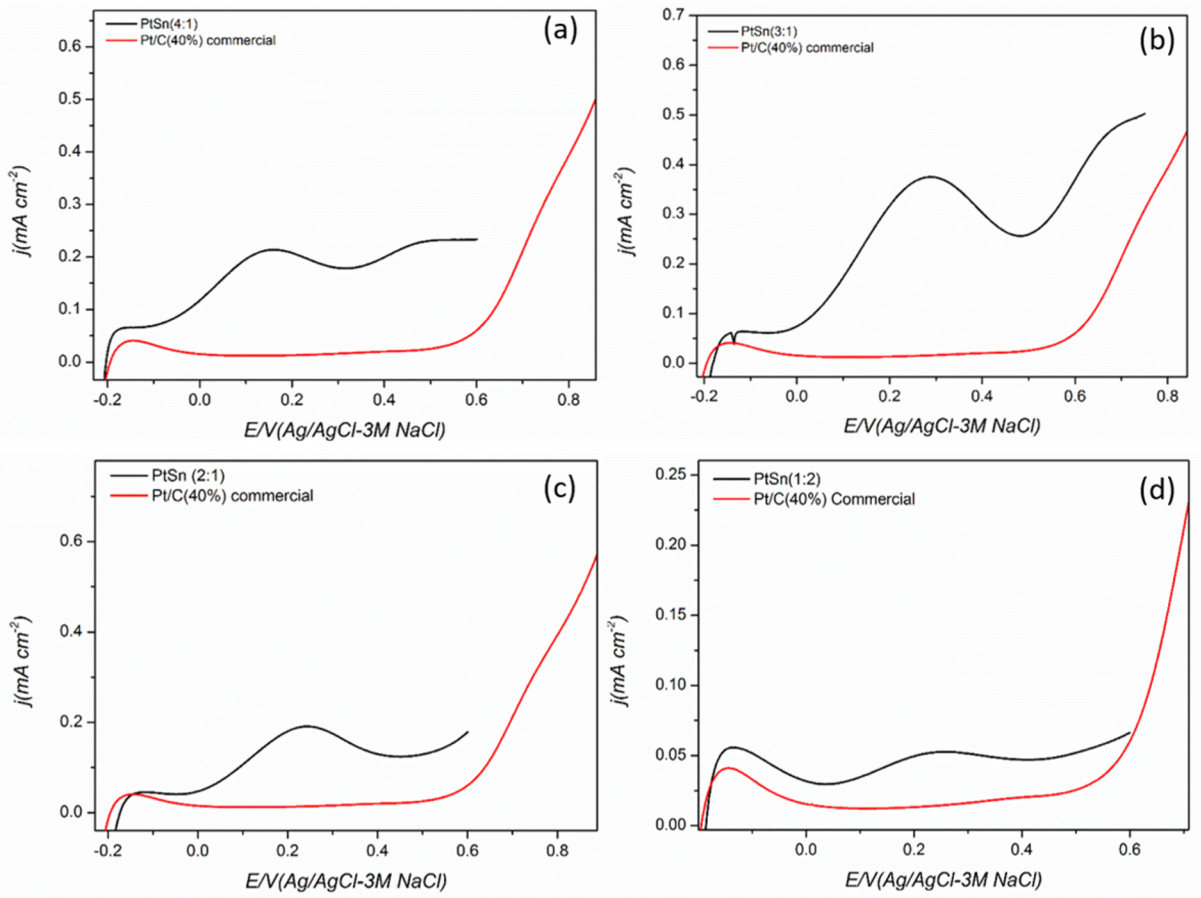

Figure 6. PGPS voltammograms of (a) PtSn(4:1), (b) PtSn(3:1), (c) PtSn(2:1), and (d) PtSn (1:2) in 0.5 M n-BtOH + 0.1 M $HClO_4$. Scan rate = 50 mV s^{-1}. The voltammogram of Pt/C (40%) commercial is also given for comparison.

of butanol showed a similar current density, indicating a similar reactivity in acidic media; whereas in alkaline media the activity of 2° isomers was lower than that of 1°, as reported in our previous study. Thus, in both media, primary butanol isomers could be considered as suitable fuels for DAFCs. In addition, both the 1° butanol isomers can be produced from biomass which makes them an attractive fuel for a sustainable energy future. The in situ FTIR data provides evidence of the effect of OH_{ads} in removing CO_{ads}, and it was concluded that the OH_{ads} is essential in the oxidation of alcohol on Pt.

To reduce the CO_{ads} poisoning effect by forming OH_{ads} at a lower potential, PtSn bimetallic catalysts/electrodes were studied, and a significant improvement in the performance was observed for the 1° isomers of butanol, with an oxidation peak at ∼0.25−0.30 V which is at a significantly lower overpotential than that on bare Pt. However, no significant effect with Sn addition to Pt was observed for 2° and 3° butanol. The higher activity on Sn addition to Pt for the 1° butanol could be attributed to the bifunctional mechanism associated with the bimetallic electrode. The higher activity for PtSn was also confirmed for carbon supported PtSn nanoparticle catalysts prepared by modifying commercial Pt/C with Sn. The peak at lower potential was also present in the PtSn/C electrode and a high activity was observed for PtSn(3:1)/C catalyst. The activation energy for butanol oxidation was also observed to be lower on PtSn(3:1)/C (∼15 kJ mol^{-1}) compared to that of Pt/C catalyst (∼37 kJ mol^{-1}).

Overall, we have successfully demonstrated that higher alcohols, especially biobutanol, have the potential to be used as fuel for DAFCs, especially on multifunctional catalysts such as PtSn. Nevertheless, a detailed further study is ongoing regarding the oxidation mechanism of butanol over bimetallic catalysts which will help in the further development of multifunctional catalysts for complete electro-oxidation of biobutanol.

■ ASSOCIATED CONTENT

Supporting Information

The Supporting Information is available free of charge on the ACS Publications website at DOI: 10.1021/acsami.6b02863.

Experimental set up of in situ FTIR, FTIR spectra of *n*-BtOH and 2-BtOH oxidation on Pt in acidic media, CVs of Pt and PtSn in 0.1 M H_2SO_4, CV of PtSn(3:1) alloy in *n*-BtOH containing solution, and Arrhenius plot of butanol oxidation on Pt/C(40%) commercial and PtSn(3:1)/C catalysts (PDF)

■ AUTHOR INFORMATION

Corresponding Authors

*E-mail: w.lin@lboro.ac.uk.
*E-mail: c.hardacre@manchester.ac.uk.

Notes

The authors declare no competing financial interest.

DOI: 10.1021/acsami.6b02863
ACS Appl. Mater. Interfaces 2016, 8, 12859−12870

■ ACKNOWLEDGMENTS

UK Catalysis Hub is kindly thanked for resources and support provided via our membership of the UK Catalysis Hub Consortium and funded by EPSRC (Grant no. EP/K014706/1). Material Chemistry Centre, Dept. of Chemistry, UCL, and Dr. Ana Jorge Sobrido, Dept. Of Chemical Engineering, UCL, are kindly acknowledged for their help and support in the TEM analysis.

■ REFERENCES

(1) Lamy, C.; Belgsir, E. M.; Léger, J. M. Electrocatalytic Oxidation of Aliphatic Alcohols: Application to the Direct Alcohol Fuel Cell (DAFC). *J. Appl. Electrochem.* **2001**, *31* (7), 799−809.

(2) Lamy, C.; Lima, A.; LeRhun, V.; Delime, F.; Coutanceau, C.; Léger, J.-M. Recent Advances in the Development of Direct Alcohol Fuel Cells (DAFC). *J. Power Sources* **2002**, *105* (2), 283−296.

(3) González, M. J.; Hable, C. T.; Wrighton, M. S. Electrocatalytic Oxidation of Small Carbohydrate Fuels at Pt−Sn Modified Electrodes. *J. Phys. Chem. B* **1998**, *102* (49), 9881−9890.

(4) Li, N.-H.; Sun, S.-G.; Chen, S.-P. Studies on the Role of Oxidation States of the Platinum Surface in Electrocatalytic Oxidation of Small Primary Alcohols. *J. Electroanal. Chem.* **1997**, *430* (1−2), 57−67.

(5) Kim, J. H.; Choi, S. M.; Nam, S. H.; Seo, M. H.; Choi, S. H.; Kim, W. B. Influence of Sn Content on PtSn/C Catalysts for Electrooxidation of C1−C3 Alcohols: Synthesis, Characterization, and Electrocatalytic Activity. *Appl. Catal., B* **2008**, *82* (1−2), 89−102.

(6) Chu, Y. H.; Shul, Y. G. Alcohol Crossover Behavior in Direct Alcohol Fuel Cells (DAFCs) System. *Fuel Cells* **2012**, *12* (1), 109−115.

(7) Dürre, P. Biobutanol: An Attractive Biofuel. *Biotechnol. J.* **2007**, *2* (12), 1525−1534.

(8) Tao, L.; He, X.; Tan, E. C. D.; Zhang, M.; Aden, A. Comparative Techno-Economic Analysis and Reviews of n-Butanol Production from Corn Grain and Corn Stover. *Biofuels, Bioprod. Biorefin.* **2014**, *8* (3), 342−361.

(9) Patakova, P.; Maxa, D.; Rychtera, M.; Linhova, M.; Fribert, P.; Muzikova, Z.; Lipovsky, J.; Paulova, L.; Pospisil, M.; Melzoch, G. S. a. K., Perspectives of Biobutanol Production and Use. In *Biofuel's Engineering Process Technology*, Bernardes, M. A. D. S., Ed.; InTech, 2011.

(10) Takky, D.; Beden, B.; Leger, J. M.; Lamy, C. Evidence for the Effect of Molecular Structure on the Electrochemical Reactivity of Alcohols: Part I. Electrooxidation of the Butanol Isomers on Noble Metal Electrodes in Alkaline Medium. *J. Electroanal. Chem. Interfacial Electrochem.* **1983**, *145* (2), 461−466.

(11) Puthiyapura, V. K.; Brett, D. J.; Russell, A. E.; Lin, W. F.; Hardacre, C. Preliminary Investigation on the Electrochemical Activity of Butanol Isomers as Potential Fuel for Direct Alcohol Fuel Cell. *ECS Trans.* **2015**, *69* (17), 809−816.

(12) Raicheva, S. N.; Christov, M. V.; Sokolova, E. I. Effect of the Temperature on the Electrochemical Behaviour of Aliphatic Alcohols. *Electrochim. Acta* **1981**, *26* (11), 1669−1676.

(13) Takky, D.; Beden, B.; Leger, J.-M.; Lamy, C. Evidence for the Effect of Molecular Structure on the Electrochemical Reactivity of Alcohols: Part II. Electrocatalytic Oxidation of the Butanol Isomers on Platinum in Alkaline Medium. *J. Electroanal. Chem. Interfacial Electrochem.* **1985**, *193* (1−2), 159−173.

(14) Takky, D.; Beden, B.; Leger, J. M.; Lamy, C. Evidence for the Effect of Molecular Structure on the Electrochemical Reactivity of Alcohols: Part III. Electro-Oxidation of the Butanol Isomers on Platinum Single Crystals in an Alkaline Medium. *J. Electroanal. Chem. Interfacial Electrochem.* **1988**, *256* (1), 127−136.

(15) Frelink, T.; Visscher, W.; van Veen, J. A. R. On the Role of Ru and Sn as Promotors of Methanol Electro-Oxidation Over Pt. *Surf. Sci.* **1995**, *335*, 353−360.

(16) Wang, K.; Gasteiger, H. A.; Markovic, N. M.; Ross, P. N., Jr On the Reaction Pathway for Methanol and Carbon Monoxide Electrooxidation on Pt-Sn Alloy versus Pt-Ru Alloy Surfaces. *Electrochim. Acta* **1996**, *41* (16), 2587−2593.

(17) Gasteiger, H. A.; Markovic, N. M.; Ross, P. N. Electrooxidation of CO and H2/CO Mixtures on a Well-Characterized Pt3Sn Electrode Surface. *J. Phys. Chem.* **1995**, *99* (22), 8945−8949.

(18) Stevanović, S.; Tripković, D.; Tripković, V.; Minić, D.; Gavrilović, A.; Tripković, A.; Jovanović, V. M. Insight into the Effect of Sn on CO and Formic Acid Oxidation at PtSn Catalysts. *J. Phys. Chem. C* **2014**, *118* (1), 278−289.

(19) Michalak, W. D.; Krier, J. M.; Alayoglu, S.; Shin, J.-Y.; An, K.; Komvopoulos, K.; Liu, Z.; Somorjai, G. A. CO Oxidation on PtSn Nanoparticle Catalysts Occurs at the Interface of Pt and Sn Oxide Domains Formed Under Reaction Conditions. *J. Catal.* **2014**, *312*, 17−25.

(20) Asgardi, J.; Calderón, J. C.; Alcaide, F.; Querejeta, A.; Calvillo, L.; Lázaro, M. J.; García, G.; Pastor, E. Carbon Monoxide and Ethanol Oxidation on PtSn Supported Catalysts: Effect of the Nature of the Carbon Support and Pt:Sn Composition. *Appl. Catal., B* **2015**, *168−169*, 33−41.

(21) Flórez-Montaño, J.; García, G.; Rodríguez, J. L.; Pastor, E.; Cappellari, P.; Planes, G. A. On the Design of Pt Based Catalysts. Combining Porous Architecture with Surface Modification by Sn for Electrocatalytic Activity Enhancement. *J. Power Sources* **2015**, *282* (0), 34−44.

(22) Tripković, A. V.; Popović, K. D.; Lović, J. D. The Influence of the Oxygen-Containing Species on the Electrooxidation of the C1−C4 Alcohols at some Platinum Single Crystal Surfaces in Alkaline Solution. *Electrochim. Acta* **2001**, *46* (20−21), 3163−3173.

(23) Jin, J. M.; Sheng, T.; Lin, X.; Kavanagh, R.; Hamer, P.; Hu, P.; Hardacre, C.; Martinez-Bonastre, A.; Sharman, J.; Thompsett, D.; Lin, W. F. Origin of High Activity but Low CO2 Selectivity on Binary PtSn Catalysts in the Direct Ethanol Fuel Cell. *Phys. Chem. Chem. Phys.* **2014**, *16*, 9432−9440.

(24) Delime, F.; Léger, J. M.; Lamy, C. Enhancement of the Electrooxidation of Ethanol on a Pt−PEM Electrode Modified by Tin. Part I: Half Cell Study. *J. Appl. Electrochem.* **1999**, *29* (11), 1249−1254.

(25) Gupta, S. S.; Singh, S.; Datta, J. Promoting Role of Unalloyed Sn in PtSn Binary Catalysts for Ethanol Electro-Oxidation. *Mater. Chem. Phys.* **2009**, *116* (1), 223−228.

(26) Vigier, F.; Coutanceau, C.; Hahn, F.; Belgsir, E. M.; Lamy, C. On the Mechanism of Ethanol Electro-oxidation on Pt and PtSn Catalysts: Electrochemical and in situ IR Reflectance Spectroscopy Studies. *J. Electroanal. Chem.* **2004**, *563* (1), 81−89.

(27) Zhou, W.-P.; Axnanda, S.; White, M. G.; Adzic, R. R.; Hrbek, J. Enhancement in Ethanol Electrooxidation by SnOx Nanoislands Grown on Pt(111): Effect of Metal Oxide−Metal Interface Sites. *J. Phys. Chem. C* **2011**, *115* (33), 16467−16473.

(28) Purgato, F. L. S.; Olivi, P.; Léger, J. M.; de Andrade, A. R.; Tremiliosi-Filho, G.; Gonzalez, E. R.; Lamy, C.; Kokoh, K. B. Activity of Platinum−Tin Catalysts Prepared by the Pechini−Adams Method for the Electrooxidation of Ethanol. *J. Electroanal. Chem.* **2009**, *628* (1−2), 81−89.

(29) Antolini, E. Catalysts for Direct Ethanol Fuel Cells. *J. Power Sources* **2007**, *170* (1), 1−12.

(30) Zhu, M.; Sun, G.; Xin, Q. Effect of Alloying Degree in PtSn Catalyst on the Catalytic behavior for Ethanol Electro-Oxidation. *Electrochim. Acta* **2009**, *54* (5), 1511−1518.

(31) Marković, N. M., The Hydrogen Electrode Reaction and the Electrooxidation of CO and H_2/CO Mixtures on Well-Characterized Pt and Pt-Bimetallic Surfaces. In *Handbook of Fuel Cells*; John Wiley & Sons, Ltd., 2010.

(32) Zhou, W. J.; Song, S. Q.; Li, W. Z.; Zhou, Z. H.; Sun, G. Q.; Xin, Q.; Douvartzides, S.; Tsiakaras, P. Direct Ethanol Fuel Cells based on PtSn Anodes: the Effect of Sn Content on the Fuel Cell Performance. *J. Power Sources* **2005**, *140* (1), 50−58.

(33) Puthiyapura, V. K.; Brett, D. J. L.; Russell, A. E.; Lin, W. F.; Hardacre, C. Development of a PtSn Bimetallic Catalyst for Direct

DOI: 10.1021/acsami.6b02863
ACS Appl. Mater. Interfaces 2016, 8, 12859−12870

Fuel Cells using Bio-Butanol Fuel. *Chem. Commun.* **2015**, *51* (69), 13412−13415.
(34) Puthiyapura, V. K.; Pasupathi, S.; Basu, S.; Wu, X.; Su, H.; Varagunapandiyan, N.; Pollet, B.; Scott, K. RuxNb1−xO2 Catalyst for the Oxygen Evolution Reaction in Proton Exchange Membrane Water Electrolysers. *Int. J. Hydrogen Energy* **2013**, *38* (21), 8605−8616.
(35) Wei, Z. D.; Li, L. L.; Luo, Y. H.; Yan, C.; Sun, C. X.; Yin, G. Z.; Shen, P. K. Electrooxidation of Methanol on upd-Ru and upd-Sn Modified Pt Electrodes. *J. Phys. Chem. B* **2006**, *110* (51), 26055−26061.
(36) Zinola, C.; Rodríguez, J. Tin Underpotential Deposition on Platinum and its Catalytic Influence on the Kinetics of Molecular Oxygen Electroreduction. *J. Solid State Electrochem.* **2002**, *6* (6), 412−419.
(37) Nan-Hai, L.; Shi-Gang, S. In situ FTIR spectroscopic Studies of the Electrooxidation of C4 Alcohol on a Platinum Electrode in Acid Solutions Part I. Reaction Mechanism of 1-Butanol Oxidation. *J. Electroanal. Chem.* **1997**, *436* (1−2), 65−72.
(38) Habibi, B.; Dadashpour, E. Electrooxidation of 2-Propanol and 2-Butanol on the Pt−Ni Alloy Nanoparticles in Acidic Media. *Electrochim. Acta* **2013**, *88* (0), 157−164.
(39) Beden, B.; Kadirgan, F.; Lamy, C.; Leger, J. M. Electrocatalytic Oxidation of Methanol on Platinum-based Binary Electrodes. *J. Electroanal. Chem. Interfacial Electrochem.* **1981**, *127* (1−3), 75−85.
(40) Gootzen, J. F. E.; Wonders, A. H.; Visscher, W.; van Veen, J. A. R. Adsorption of C3 Alcohols, 1-Butanol, and Ethene on Platinized Platinum As Studied with FTIRS and DEMS. *Langmuir* **1997**, *13* (6), 1659−1667.
(41) Iwasita, T.; Pastor, E. A Dems and FTIR Spectroscopic Investigation of Adsorbed Ethanol on Polycrystalline Platinum. *Electrochim. Acta* **1994**, *39* (4), 531−537.
(42) Pastor, E.; Wasmus, S.; Iwasita, T.; Arévalo, M. C.; González, S.; Arvia, A. J. Spectroscopic Investigations of C3 Primary Alcohols on Platinum Electrodes in Acid Solutions.: Part I. n-Propanol. *J. Electroanal. Chem.* **1993**, *350* (1−2), 97−116.
(43) Katikawong, P.; Ratana, T.; Veerasai, W. Temperature Dependence Studies on the Electro-oxidation of Aliphatic Alcohols with Modified Platinum Electrodes. *J. Chem. Sci.* **2009**, *121* (3), 329−337.
(44) Yáñez, C.; Gutiérrez, C.; Ureta-Zañartu, M. S. Electrooxidation of Primary Alcohols on Smooth and Electrodeposited Platinum in Acidic Solution. *J. Electroanal. Chem.* **2003**, *541* (0), 39−49.
(45) Razmi, H.; Habibi, E.; Heidari, H. Electrocatalytic Oxidation of Methanol and Ethanol at Carbon Ceramic Electrode Modified with Platinum Nanoparticles. *Electrochim. Acta* **2008**, *53* (28), 8178−8185.
(46) Chen, S.; Schell, M. Excitability and Multistability in the Electrochemical Oxidation of Primary Alcohols. *Electrochim. Acta* **2000**, *45* (19), 3069−3080.
(47) Fujiwara, N.; Friedrich, K. A.; Stimming, U. Ethanol Oxidation on PtRu Electrodes Studied by Differential Electrochemical Mass Spectrometry. *J. Electroanal. Chem.* **1999**, *472* (2), 120−125.
(48) Wang, H.; Jusys, Z.; Behm, R. J. Ethanol Electrooxidation on a Carbon-Supported Pt Catalyst: Reaction Kinetics and Product Yields. *J. Phys. Chem. B* **2004**, *108* (50), 19413−19424.
(49) Lee, C.-G.; Umeda, M.; Uchida, I. Cyclic Voltammetric Analysis of C1−C4 Alcohol Electrooxidations with Pt/C and Pt−Ru/C Microporous Electrodes. *J. Power Sources* **2006**, *160* (1), 78−89.
(50) Sen Gupta, S.; Datta, J. An Investigation into the Electro-Oxidation of Ethanol and 2-Propanol for Application in Direct Alcohol Fuel Cells (DAFCs). *Proc. - Indian Acad. Sci., Chem. Sci.* **2005**, *117* (4), 337−344.
(51) Hilmi, A.; Belgsir, E. M.; Léger, J. M.; Lamy, C. Electrocatalytic Oxidation of Aliphatic Diols on Platinum and Gold Part I: Effects of Chain Length and Isomeric Position. *J. Electroanal. Chem.* **1995**, *380* (1−2), 177−184.
(52) Rodrigues, I. d. A.; De Souza, J. P. I.; Pastor, E.; Nart, F. C. Cleavage of the C−C Bond during the Electrooxidation of 1-Propanol and 2-Propanol: Effect of the Pt Morphology and of Codeposited Ru. *Langmuir* **1997**, *13* (25), 6829−6835.
(53) Gojković, S. L.; Tripković, A. V.; Stevanović, R. M. Mixtures of Methanol and 2-Propanol as a Potential Fuel for Direct Alcohol Fuel Cells. *J. Serb. Chem. Soc.* **2007**, *72* (12), 1419−1425.
(54) Pastor, E.; González, S.; Arvia, A. J. Electroreactivity of Isopropanol on Platinum in Acids Studied by DEMS and FTIRS. *J. Electroanal. Chem.* **1995**, *395* (1−2), 233−242.
(55) Sun, S.-G.; Lin, Y. In Situ FTIR Spectroscopic Investigations of Reaction Mechanism of Isopropanol Oxidation on Platinum Single Crystal Electrodes. *Electrochim. Acta* **1996**, *41* (5), 693−700.
(56) Otomo, J.; Li, X.; Kobayashi, T.; Wen, C.-j.; Nagamoto, H.; Takahashi, H. AC-Impedance Spectroscopy of Anodic Reactions with Adsorbed Intermediates: Electro-Oxidations of 2-Propanol and Methanol on Carbon-Supported Pt Catalyst. *J. Electroanal. Chem.* **2004**, *573* (1), 99−109.
(57) Wang, J.; Wasmus, S.; Savinell, R. F. Evaluation of Ethanol, 1-Propanol, and 2-Propanol in a Direct Oxidation Polymer-Electrolyte Fuel Cell: A Real-Time Mass Spectrometry Study. *J. Electrochem. Soc.* **1995**, *142* (12), 4218−4224.
(58) Wang, Y.; Mi, Y.; Redmon, N.; Holiday, J. Understanding Electrocatalytic Activity Enhancement of Bimetallic Particles to Ethanol Electro-oxidation. 1. Water Adsorption and Decomposition on PtnM (n = 2, 3, and 9; M = Pt, Ru, and Sn). *J. Phys. Chem. C* **2010**, *114* (1), 317−326.
(59) Lamy-Pitara, E.; Ouazzani-Benhima, L. E.; Barbier, J.; Cahoreau, M.; Caisso, J. Adsorption of Tin on Platinum: an Uncommon Underpotential Deposition. *J. Electroanal. Chem.* **1994**, *372* (1−2), 233−242.
(60) Hable, C. T.; Wrighton, M. S. Electrocatalytic Oxidation of Methanol by Assemblies of Platinum/Tin Catalyst Particles in a Conducting Polyaniline Matrix. *Langmuir* **1991**, *7* (7), 1305−1309.
(61) Li, H.; Sun, G.; Cao, L.; Jiang, L.; Xin, Q. Comparison of Different Promotion Effect of PtRu/C and PtSn/C Electrocatalysts for Ethanol Electro-Oxidation. *Electrochim. Acta* **2007**, *52* (24), 6622−6629.
(62) Beyhan, S.; Coutanceau, C.; Léger, J.-M.; Napporn, T. W.; Kadırgan, F. Promising Anode Candidates for Direct Ethanol Fuel Cell: Carbon Supported PtSn-based Trimetallic Catalysts prepared by Bönnemann Method. *Int. J. Hydrogen Energy* **2013**, *38* (16), 6830−6841.
(63) Lim, D.-H.; Choi, D.-H.; Lee, W.-D.; Lee, H.-I. A New Synthesis of a Highly Dispersed and CO Tolerant PtSn/C Electrocatalyst for Low-Temperature Fuel Cell; its Electrocatalytic Activity and Long-Term Durability. *Appl. Catal., B* **2009**, *89* (3−4), 484−493.
(64) Nam, S. C.; Yoon, Y. S.; Cho, W. I.; Cho, B. W.; Chun, H. S.; Yun, K. S. Reduction of Irreversibility in the First Charge of Tin Oxide Thin Film Negative Electrodes. *J. Electrochem. Soc.* **2001**, *148* (3), A220−A223.
(65) Lee, K.-M.; Lee, D.-J.; Ahn, H. XRD and TEM Studies on Tin Oxide (II) Nanoparticles Prepared by Inert Gas Condensation. *Mater. Lett.* **2004**, *58* (25), 3122−3125.
(66) Mukerjee, S.; McBreen, J. An In Situ X-Ray Absorption Spectroscopy Investigation of the Effect of Sn Additions to Carbon-Supported Pt Electrocatalysts: Part I. *J. Electrochem. Soc.* **1999**, *146* (2), 600−606.
(67) Kibler, L. A. Hydrogen Electrocatalysis. *ChemPhysChem* **2006**, *7* (5), 985−991.
(68) Kibler, L. A.; El-Aziz, A. M.; Hoyer, R.; Kolb, D. M. Tuning Reaction Rates by Lateral Strain in a Palladium Monolayer. *Angew. Chem., Int. Ed.* **2005**, *44* (14), 2080−2084.
(69) Silva, J. C. M.; Parreira, L. S.; De Souza, R. F. B.; Calegaro, M. L.; Spinacé, E. V.; Neto, A. O.; Santos, M. C. PtSn/C Alloyed and Non-Alloyed Materials: Differences in the Ethanol Electro-oxidation Reaction Pathways. *Appl. Catal., B* **2011**, *110*, 141−147.
(70) Sen Gupta, S.; Singh, S.; Datta, J. Temperature Effect on the Electrode Kinetics of Ethanol Electro-Oxidation on Sn Modified Pt Catalyst through Voltammetry and Impedance Spectroscopy. *Mater. Chem. Phys.* **2010**, *120* (2−3), 682−690.

DOI: 10.1021/acsami.6b02863
ACS Appl. Mater. Interfaces 2016, 8, 12859−12870